

This article was downloaded by:

On: 22 January 2011

Access details: *Access Details: Free Access*

Publisher *Taylor & Francis*

Informa Ltd Registered in England and Wales Registered Number: 1072954 Registered office: Mortimer House, 37-41 Mortimer Street, London W1T 3JH, UK



The Journal of Adhesion

Publication details, including instructions for authors and subscription information:

<http://www.informaworld.com/smpp/title~content=t713453635>

Stress Transfer in Single Fiber/ Resin Tensile Tests

W. D. Bascom^a; R. M. Jensen^a

^a Hercules Aerospace, Magna, Utah, U.S.A.

To cite this Article Bascom, W. D. and Jensen, R. M.(1986) 'Stress Transfer in Single Fiber/ Resin Tensile Tests', The Journal of Adhesion, 19: 3, 219 – 239

To link to this Article: DOI: 10.1080/00218468608071225

URL: <http://dx.doi.org/10.1080/00218468608071225>

PLEASE SCROLL DOWN FOR ARTICLE

Full terms and conditions of use: <http://www.informaworld.com/terms-and-conditions-of-access.pdf>

This article may be used for research, teaching and private study purposes. Any substantial or systematic reproduction, re-distribution, re-selling, loan or sub-licensing, systematic supply or distribution in any form to anyone is expressly forbidden.

The publisher does not give any warranty express or implied or make any representation that the contents will be complete or accurate or up to date. The accuracy of any instructions, formulae and drug doses should be independently verified with primary sources. The publisher shall not be liable for any loss, actions, claims, proceedings, demand or costs or damages whatsoever or howsoever caused arising directly or indirectly in connection with or arising out of the use of this material.

Stress Transfer in Single Fiber/ Resin Tensile Tests

W. D. BASCOM and R. M. JENSEN

Hercules Aerospace, Magna, Utah 84044-0098, U.S.A.

(Received March 3, 1985; in final form October 1, 1985)

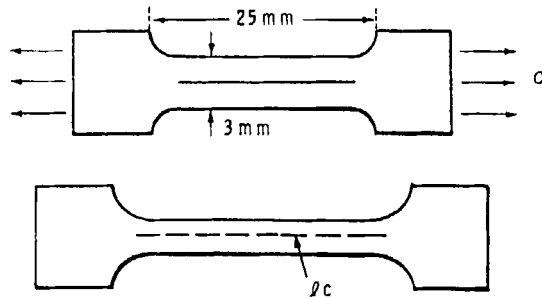
Microscale (25 mm gauge length) "dogbone" resin specimens with single carbon fibers embedded through the length of the specimen have been studied as a method for determining the fiber-resin interphase strength. The specimens are pulled in tension until the fiber fragments to a critical length, l_c . Evidence is presented here, based primarily on the relaxation of stress birefringence around the fiber fragment, that this test may not be an unambiguous measure of fiber-resin adhesion. Data obtained for various production lots of AS-4, AS-6, and IM-6 fibers indicate an increase in l_c/d with laminate tensile strength. Although there is theoretical justification for this correlation, it requires that the interphase shear strength is relatively constant.

In those instances where interfacial adhesion was expected to be low, *i.e.*, surface contamination or unsurface treated fiber, there was a significant increase in l_c/d and usually a distinct difference in stress birefringence compared to "good" adhesion. However, the distinction in stress birefringence was not always clear cut.

KEY WORDS Adhesion; Composites; Interphase strength; Single fiber/resin specimen; Stress transfer; Tensile testing.

INTRODUCTION

A number of studies have been made of the tensile behavior of single fibers, primarily carbon and glass, embedded in micro-size (25 mm gauge length) resin dogbones. As originally described by Kelly,¹ the fiber should break into fragments as tensile load is applied to the specimen until a limiting fragment size, l_c , is reached which is too short to allow the transfer of stress equal or greater than the fiber tensile strength, σ_c . A schematic of the specimen is



$$\tau = \frac{\sigma_c}{2} \left(\frac{d}{l_c} \right)$$

FIGURE 1 Schematic of single fiber micro-dogbone specimens (See text for symbols).

given in Figure 1. Kelly¹ derived a relatively simple expression relating l_c , σ_c , the shear stress, τ_c , at the fiber resin boundary and the fiber diameter, d ;

$$\tau_c = \frac{\sigma_c d}{2l_c} \quad (1)$$

The derivation assumes a uniform fiber strength (and diameter) which, for strong brittle fibers, is generally not the case.

Kelly identified the quantity τ as the "failure stress in shear of the interface or the matrix".¹ However, there has been a tendency to equate τ with the fiber/resin interfacial shear strength. It is important to recognize that unless it can be shown independently that stress transfer is in fact limited by the interfacial strength, τ_c cannot be unequivocally identified as a measure of fiber/resin adhesion. Frazer^{2,3} *et al.* have used the single-fiber/resin specimen to study glass fiber/resin interaction. They avoid the question of the locus of stress transfer by referring to τ as the "stress transfer coefficient".

The most extensive studies of single fiber/resin tensile specimens have been by Drzal and co-workers.^{4,5} Their work has been restricted almost entirely to carbon fibers in epoxy resins and they have taken advantage of the stress birefringence of the epoxy resin to observe the stress distribution associated with fiber fracture and

shear failure between fiber and resin. This work in combination with Drzal's work on the surface properties of carbon fibers^{6,7} represents one of the most comprehensive investigations of the interfacial aspects of carbon reinforced composites.

In the work reported here, techniques similar to those devised by Drzal were used to investigate carbon single-fiber/epoxy stress transfer. Although the experimental results are in many ways similar to those of Drzal, there are some critical differences in interpretation. Notably, the identification of τ_c as an interfacial shear strength is not unequivocal. In fact, it is possible that stress transfer is limited by the shear yield strength of the resin. Further, it is shown that a rough correlation exists between the 0° laminate tensile strength and the critical fiber length when τ_c is relatively constant.

EXPERIMENTAL

Small dogbone shaped specimens were mounted in a hand-driven tensile testing machine set on the stage of a microscope. The dogbone dimensions are given in Figure 1. A photograph of the tensile tester is given in Figure 2. During testing the specimen is

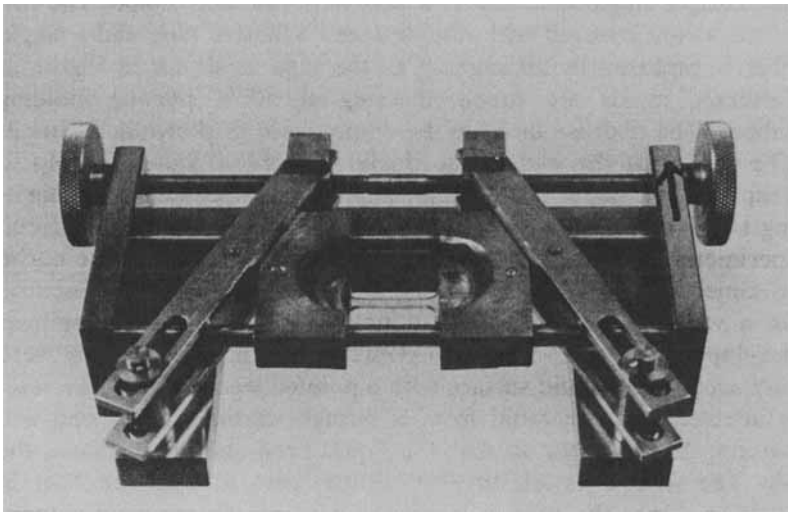


FIGURE 2 Micro-tensile test device.

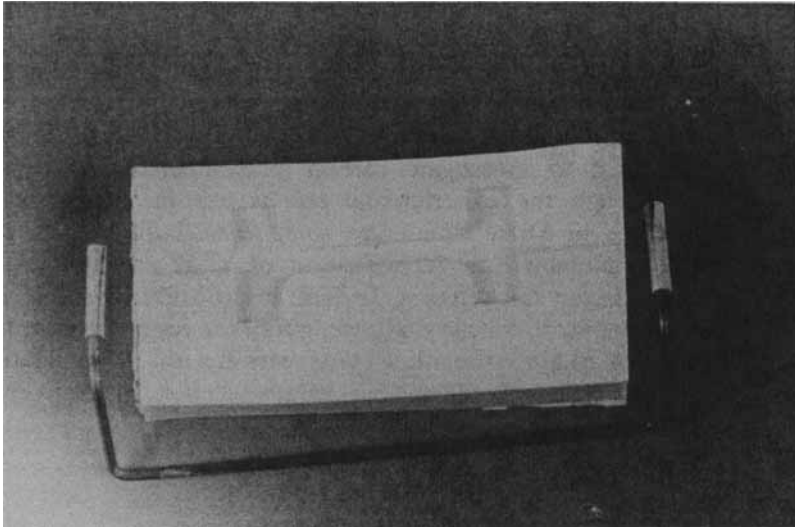


FIGURE 3 Single fiber positioned in dogbone mold.

viewed between crossed polarizing filters. The dogbone is made by mounting a single fiber across a wire bent into a U shape. The tips of the U are covered with double faced adhesive tape and a single fiber is captured by attachment to the tape as shown in Figure 3. Dogbone molds are prepared using an RTV silicone molding rubber. The fiber is placed in the empty mold as shown in Figure 3. The screws at the end of the dogbone mold, (Figure 3), help to keep the fiber centered. A major experimental problem is eliminating small air bubbles from the molding. Any bubble in the cured specimen is almost always a site for premature failure of the entire specimen. A procedure of outgassing the resin and curative mixture on a vacuum evaporator was adopted. Also, bubbles sometimes developed when the resin was poured into the mold. These were displaced to the liquid surface with a pointed wooden rod. The resin is injected into the mold from a syringe starting at one end and working to the other so that the liquid progressively displaces the air. The wire U is left in place during cure to hold the fiber in position. Once the resin is cured the wire can be removed without disturbing the embedded fiber.

Two important aspects of specimen preparation are avoiding spurious contamination of the fiber and obtaining as broad a sample population as possible. Surface contamination comes primarily from the wrapping (plastic or paper) normally put on production spools of fiber, room aerosols that deposit on unprotected spools, and in manipulating individual filaments. A procedure was established in which all fiber tow that has been in contact with the wrapping (or exposed to airborne contamination) was removed from the spool before taking a test sample. The individual fibers were removed from a tow with minimum possible handling; usually a fiber end was captured with tweezers and the fiber laid onto the wire holder so that the embedded section was never contacted by the tweezers or the operator's fingers. In addition, sample preparation was done in as clean a laboratory area as possible.

Two sources of contamination could not be conveniently eliminated; low MW silicone polymers from the molding compound and surface active materials from the adhesive tape on the U-shaped wire holder. The molds were thoroughly heat cured to reduce unreacted polymer (alternate materials such as PTFE or metal molds proved to be impractical). There was no evidence of contamination from the adhesive tape but this concern could not be eliminated.

The usual sampling procedure was to take one spool (1–3 kgm) at random from a production lot and unwrap the tow (12 K filaments) down to unexposed fiber as described above. Single filaments (12–14) were removed at about one meter intervals along the tow. This procedure could be made more representative by taking filaments from more than one spool. However, to do so would add significantly to testing costs.

The resins used in the single fiber experiments included a diglycidyl ether of Bisphenol A (DGEBA, Shell 828) cured with meta-phenylene diamine (m-PDA) or a polyoxypropylene diamine (Jefferson Chemical Co., D230). All reagents were used as received but were kept in closed, dry containers stored away from direct light. The 828/m-PDA contained 14 phr of amine and the 828/D230 contained 30 phr of amine. The cure conditions for both systems were two hours at 75°C followed by three hours at 125°C in a noncirculating oven.

Hercules resin HBRF 55A was also used. It is a DGEBA epoxy

TABLE I
Nominal properties of carbon fibers

Fiber designation	Diameter d μm	0° Laminate tensile properties		
		Strength ksi/MPa	Modulus Msi/GPa	Elongation %
AS-1	8.0	450/3103	33/228	1.32
AS-4	6.96	520/3587	34/235	1.53
AS-6	5.52	600/4173	35.3/243	1.65
IM-6	5.20	635/4378	40.4/278	1.50

cured with a mixture of aromatic amines. This resin was cured at 94°C for two hours followed by 120°C for four hours.

Laminate tensile data were obtained using unidirectional (°) 8 ply laminates fabricated from Hercules 3501-5A prepreg and autoclave cured at 177°C for two hours. They were tested at ~25°C at about 1.25 cm/min.

The fibers tested included three commercial Hercules carbon fibers, AS-4, AS-6G and IM-6G as well as a few tests on experimental fibers produced on commercial scale equipment. The pertinent data on these fibers, tested in 3501-5A, are presented in Table I.

RESULTS

Stress birefringence observations

Viewed between crossed-polarizing filters and using polychromatic light the entire epoxy specimen exhibits a sequence of birefringence colors as the specimen is initially stressed. Once the fiber begins to fracture a characteristic birefringence pattern develops at the broken fiber ends as shown in Figure 4A. As the tensile stress is increased the fiber continues to break but at the same time, the birefringence pattern around the initial breaks undergoes a distinct change. The initial birefringence nodes, clearly evident in Figure 4A, move along the fiber away from the break and leave a more-or-less uniform sheath of birefringence surrounding the fiber (Figure 4B). This phenomena slows considerably but does not cease immediately when loading is stopped (Figure 4C).

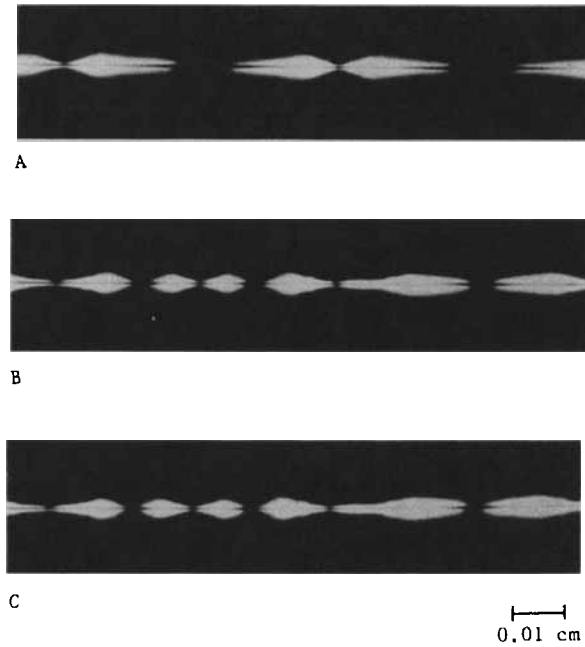


FIGURE 4 Stress birefringence pattern at initial break (A), after increasing tension (B), and tension held constant (C) (828/m-PDA).

Fiber breakage is essentially complete within a small range of tensile strain.[†] Once the fiber has been completely fractured, further loading simply caused the birefringent nodes to retreat further from the fiber breaks and thereby increase the length of the sheath between the node and break.

Removing the specimen from the test device, and thereby releasing the applied tension, caused dramatic changes in the birefringence pattern. As the sequence of photographs in Figure 5 show, the birefringence associated with the initial nodal patterns disappears but the sheath of birefringence persists. The photograph shown in Figure 5B was taken after 2 hours of relaxation but the specimen exhibited the same photostress pattern when examined

[†]The test device used in this study did not have a stress-strain read-out. Differences in strain level were qualitatively judged by the turns on the knob used to apply load.

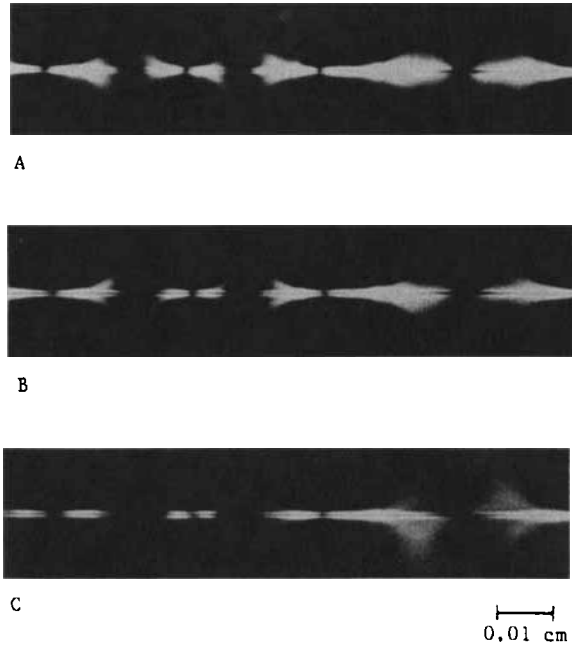


FIGURE 5 Change in stress birefringence immediately after removing tension (A), after 1-2 hr. (B) and after six months (C) (828/m-PDA).

months later (Figure 5C). These birefringent patterns and changes in birefringence with changes in stress state were observed for all of the test resins, 828/m-PDA, 828/D230 and HBRF 55A.

A very different sequence of birefringence patterns was observed for a silicon carbide (SiC) fiber where there is poor fiber-resin adhesion (presumably due to a cohesively weak surface coating). The sequence of photographs in Figure 6 shows an essentially uniform distribution of stress around the fiber extending from both sides of the fiber break. Increased stress increased the diameter of the birefringent zone (Figure 6B) but there was no evidence of the development of a sheath of birefringence as in Figure 5. Relaxation of the tensile load caused essentially all of the birefringence to dissipate (Figure 7) except at the tips of the broken ends.

The fiber shown in Figures 4 and 5 had been taken from a production lot of AS-4 and had received the usual surface treatment

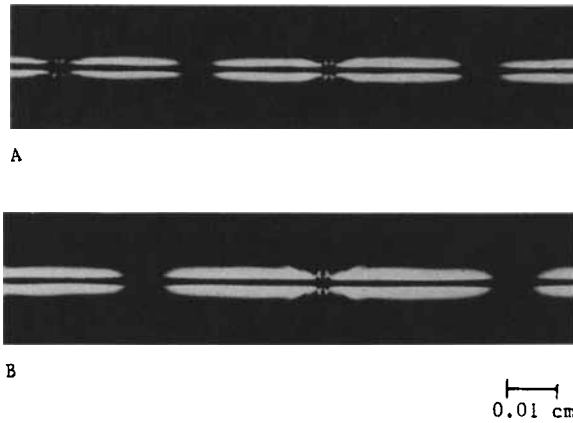


FIGURE 6 Stress birefringence exhibited by SiC fiber near breaks and in tension (828/D230).

to improve fiber-resin “adhesion” usually measured as a laminate shear strength—short beam shear.⁸ Fibers from a spool of unsurface treated fiber (AU-4) were tested and exhibited a somewhat different stress birefringence behavior as shown in Figure 8.

Initially the filament break exhibits the characteristic double node birefringence (Figure 8A). With increasing strain these nodes recede

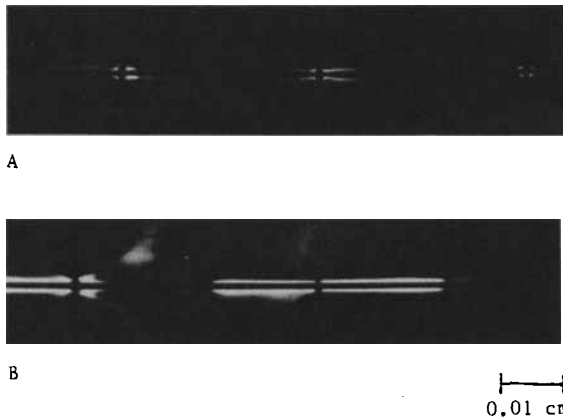


FIGURE 7 Change in birefringence around SiC fiber breaks after removing tension; (A) within 1 hr., (B) after 24 hrs. (828/D230).

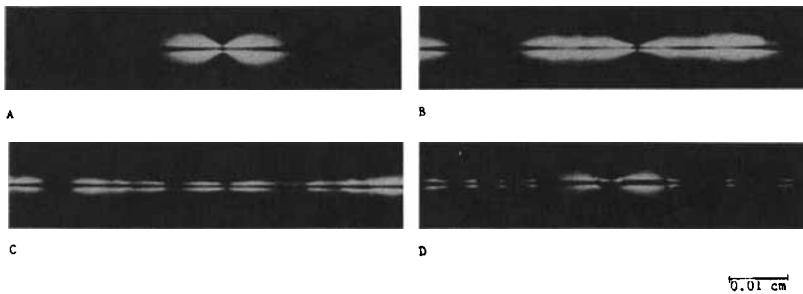


FIGURE 8 Stress birefringence patterns characteristic of unsurface treated fiber; in tension (A–C), tension relaxed (D) (828/m-PDA).

from the fiber ends and leave a tongue of birefringence (Figure 8B) similar to the pattern for surface treated fibers (Figure 4). A further increase in strain causes the birefringence to break up into a series of bright streaks distributed (unevenly) on both sides of the break (Figure 8C). At the same time the initial nodes recede from the fiber ends. This redistribution of the birefringence occurs with only a slight increase in stress over that required for fiber fracture. Relaxation of the tension on the specimen causes the birefringence to dissipate except for residual streaks near the fiber break and at discrete intervals along the fiber on both sides of the break (Figure 8D). Drzal has reported similar behavior for for AU-4 fiber in m-PDA/828.⁵

These relaxation experiments suggest that for “good” adhesion, the birefringence node corresponds to elastic deformation of the resin due to the high stress concentration at the fiber ends. Imposing additional tensile stress on the specimen causes shear failure of the resin along the fiber; the sheath of birefringence that develops as the original node moves away from the break. The fact that the node dissipates almost immediately after removing the tensile stress indicates recoverable elastic strain. The persistence of the birefringent sheath, even months after removing the tensile load, indicates plastic (nonrecoverable) shear deformation of the resin that extends at least one fiber diameter around the fiber.

In the case of “poor” fiber/resin adhesion—the SiC/828-D230 system—relaxation causes essentially all of the birefringence to dissipate. Presumably, the stress developed under tension is the result of frictional forces between fiber and resin which are sufficient

to cause elastic deformation of the resin but too low to cause shear yielding.

The AU-4 fiber behavior (Figure 8) appears to represent an intermediate situation between "good" and "poor" adhesion. Initially, the high shear stress at the fiber ends produces the expected nodal birefringence followed by shear yielding of the resin around the fiber. However, because of variations in bond strength along the fiber surface, this yielding precedes in a slip-stick fashion leaving streaks of birefringence where the adhesion strength was sufficient to cause plastic deformation of the resin interrupted by areas of interfacial failure (or possibly cohesive failure in the fiber surface).

Critical aspect ratio

The fiber fragment lengths, l_c , were measured for a number of carbon fiber/resin compositions. In each test, load was applied until it was certain that the fiber had fully fragmented. The variation in the l_c data is very broad so that the results must be treated statistically. Typical distributions in l_c for a single test are shown in Figure 9 as a histogram with a normal distribution overlay and in

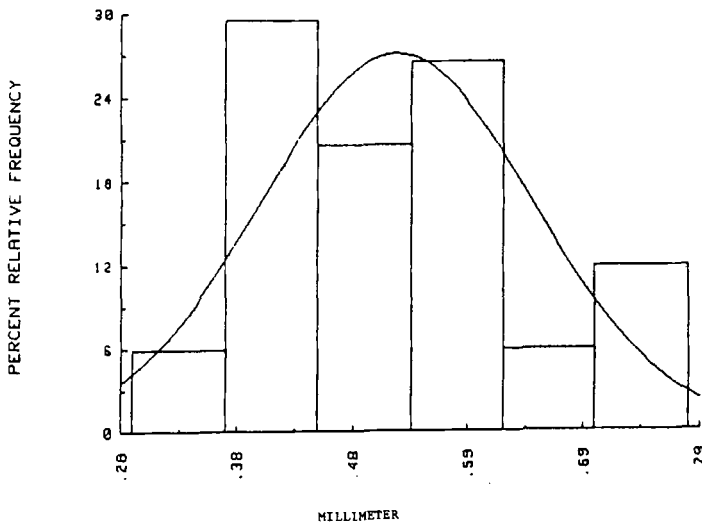


FIGURE 9 Histogram and normal curve overlay for l_c from one dogbone test.

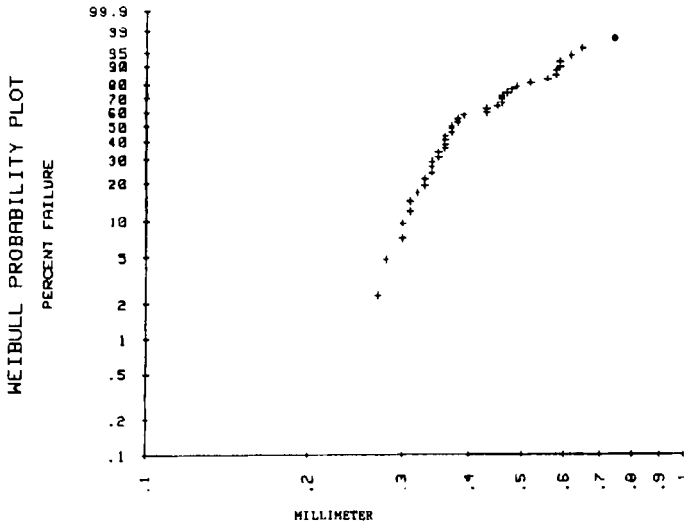


FIGURE 10 Typical l_c data from one dogbone test presented as a Weibull distribution.

Figure 10 as a two parameter Weibull plot. Because of the large data scatter a procedure was adopted to test 10–12 specimens for each fiber-resin combination and combine the l_c data for statistical analysis and comparisons. The graphical distributions for data from multiple tests are shown in Figures 11 and 12.

Other workers^{5,7} have elected to treat l_c data using Weibull statistical treatments. However, as shown in Figure 12, the data do not give the linear Weibull plot expected for a two parameter Weibull distribution. In fact, the data for a single specimen (Figure 10) appear to be grouped into separate, linear segments. The applications of the two parameter Weibull statistics to brittle failure usually assumes failure initiates at one type of flaw. The discontinuities in Figure 10 and the distinct curvature of the combined data in Figure 12 suggests that fiber fracture is initiated by different types of flaws.

Because of the uncertainties in using Weibull statistics, analysis of the l_c data in this report was restricted to comparisons of the normal means; more specifically to the 99% confidence on the mean interval. The data for various lots of production AS-4 fiber in the

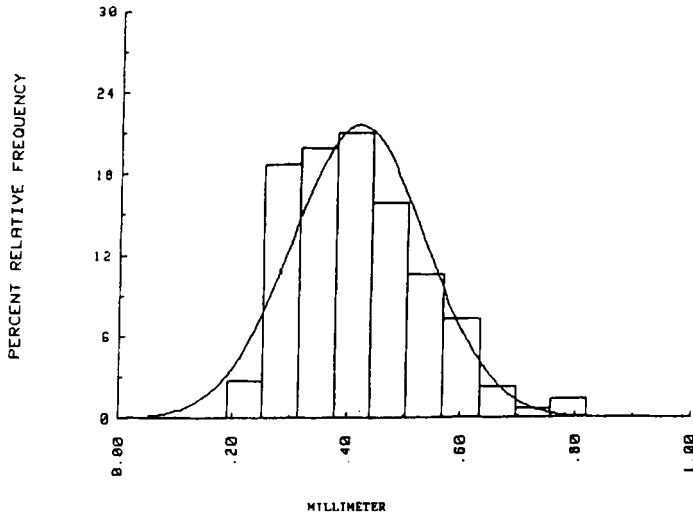


FIGURE 11 Histogram and normal overlay for combined l_c data from 10 specimens.

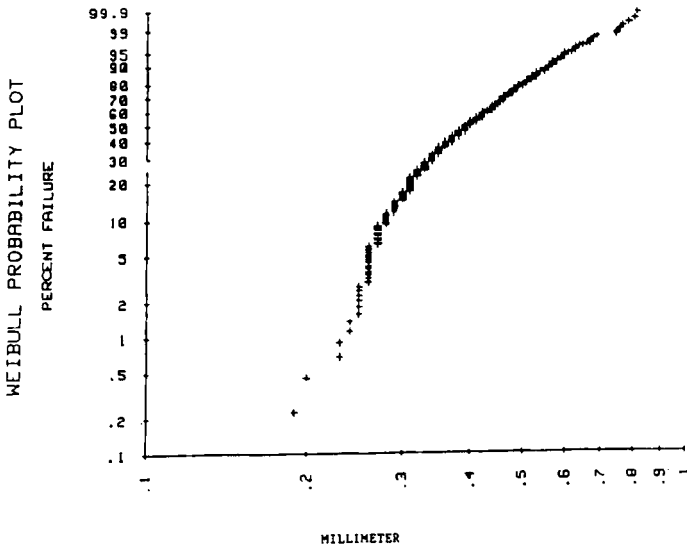


FIGURE 12 Typical l_c data for 10 specimens presented as a Weibull distribution.

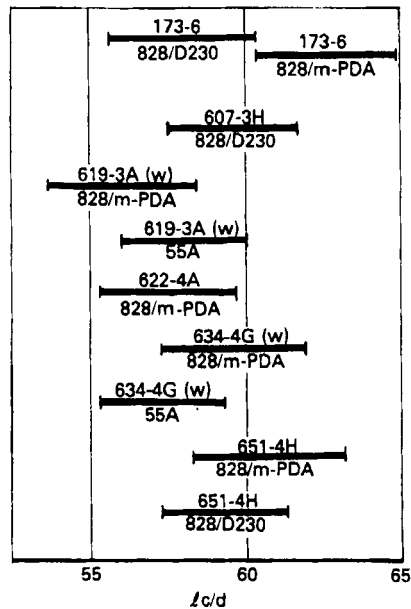


FIGURE 13 Confidence limits (99%) on l_c/d for AS-4/resin systems.

three test resins are presented in Figure 13. For later comparisons with fibers having different diameters the data are plotted as l_c/d , the critical aspect ratio. Each line represents the 99% confidence interval with the fiber lot number indicated above the line and the test resin below the line. Some fibers had been sized with Hercules W-size and are so indicated by (W) after the lot number. A nominal fiber diameter was assumed (Table I) but it is recognized that there is a small variation in diameter which contributes to the variation in l_c/d .

Clearly, the data intervals in Figure 13 are not identical but there are no systematic differences with respect to the three test resins, fiber sizing or the period of fiber production which covered three years starting in mid 1981 with Lot 173-6.

The effect of fiber surface treatment on l_c/d is shown in Figure 14. Two lots of 'unsurface treated fiber, AU-4, Lot 173-6 and Lot 640-4L are compared with surface treated fiber, AS-4, from the same production run in one case (173-6) or lots produced within a

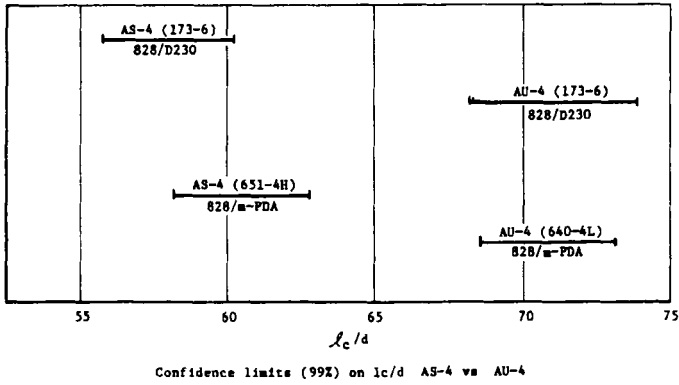


FIGURE 14 Confidence limits (99%) on l_c/d for AS-4 fiber vs AU-4 fiber.

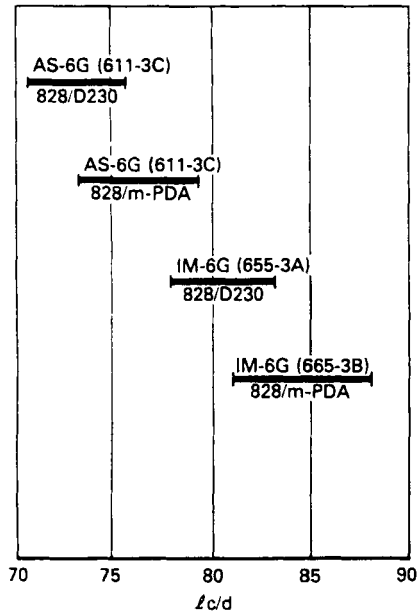


FIGURE 15 Confidence limits (99%) on l_c/d for AS-6G and IM-6G.

months time (640-4L vs 651-4H). In both cases the AU-4 fiber exhibited significantly higher l_c/d values than the surface treated fibers.

Presumably, this difference in critical fiber length is due to poor adhesion of the unsurface treated fiber, *i.e.*, lower τ_c in Eq. (1). However, neither sample of AU-4 gave a birefringence pattern that was clearly indicative of "poor" adhesion, *i.e.*, the pattern obtained with the SiC fiber. In fact, all test specimens of the AU-4 from Lot 640-4L showed the "intermediate" stress pattern, *i.e.*, Figure 8. Fibers from Lot 173-6 (AU-4) exhibited birefringence patterns characteristic of good adhesion (Figure 4) in 22 out of 24 specimens, the other two showed the "intermediate" pattern.

The l_c/d results for Hercules AS-6G and IM-6G are presented in Figure 15. All fibers had been sized with the epoxy compatible G-size. The range in l_c/d for the AS-6G and IM-6G are significantly higher than for the AS-4 fiber. In all cases the birefringence pattern indicated, "good" adhesion.

DISCUSSION

The results presented here are most easily discussed if Eq. (1) is rearranged to:

$$\frac{l_c}{d} = \frac{\sigma_c}{2\tau_c} \quad (2)$$

which points up the fact that *both* an increase in fiber strength, σ_c , or decrease in τ_c increase the critical aspect ratio. Consequently, it is not possible to use l_c/d data to test for differences in fiber strength or fiber-resin adhesion without some independent evidence that either σ_c or τ_c is invariant.

In using Eq. (2) to determine τ_c it is necessary to determine σ_c independently. Moreover, the fiber strength varies with test length and, for a given length has a wide statistical distribution. The appropriate value for σ_c in Eq. (2) would be at or near the average critical length, l_c . In the work by Drzal^{4,5} they were able to determine σ_c for very short (0.1-1.0 mm) fiber lengths and used the mean strength σ_c to compute τ_c . Alternatively, Eq. (2) can be recast into a statistical format⁹ that accounts for the distribution in l_c and τ_c .

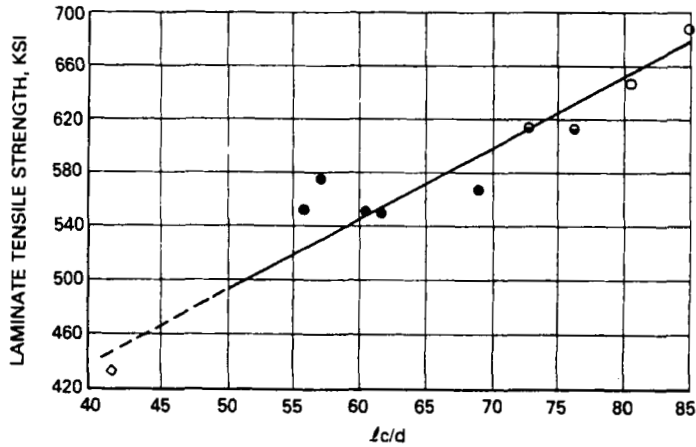


FIGURE 16 Correlation of average l_c/d with laminate 0° tensile strength (fiber lot acceptance data); AS-1, AS-4, AS-6, IM-6.

In the work reported here it was not possible to measure σ_c at short fiber lengths so that the l_c/d data were not converted to τ_c .

Equation 2 suggests that the critical aspect ratio can be correlated with fiber tensile strength if τ_c is relatively constant. In Figure 16 a plot of l_c/d against 0° laminate tensile strength¹⁰ gives a reasonably linear correlation. In this plot the l_c/d data were selected for systems that exhibited "good" adhesion as judged by the birefringence pattern, *i.e.* Figure 4. The critical length data include results for three different resins and sized and unsized fiber. Presumably, the variation in τ_c is small compared to the differences in tensile strength and critical length. Very likely this is a fortuitous coincidence because the resins and sizing agents are chemically similar and/or the fibers received similar surface treatments.

The 0° laminate tensile strength reflects single fiber strengths, σ_c , albeit the relationship is indirect and poorly understood in any quantitative sense; single fibers and 0° laminates fail by different modes.

The fact that a linear correlation was obtained in Figure 16 indicates that if τ_c is relatively constant then the critical aspect ratio is largely determined by the fiber tensile strength. Stated differently, the progressive increase in fiber strength between AS-1 and IM-6 is the result of a decrease in the type and distribution of surface and

internal (macroscopic) flaws. As the average distance between flaws increases the minimum distance between breaks (l_c) increases in the single fiber test. If the bonding between the fiber and resin is "poor" or the shear strength of the resin is too low to "test" the stronger flaws, then a simple correlation between fiber (or laminate) strength is likely to break down. For example, data for unsurface treated fiber (AU-4) do not fit the plot in Figure 16. (In this case there has been a large change in τ_c .) On the other hand, as carbon fibers are developed with increasing tensile strength the resins used here for single fiber tests may be too weak in shear to determine the fibers "usable" critical length. Indeed, the merit of plots such as Figure 16 is for fiber characterization.

The single fiber test is often viewed as a test for the interfacial shear strength between fiber and matrix. Actually, there is no fundamental basis for identifying τ_c as an interfacial parameter unless there is some independent evidence that failure occurs precisely at the boundary between the two phases. In fact, it is usually difficult to identify the interface between two solids and many authors, notably Sharpe,¹¹ have suggested that for most real systems the boundary between two solids be viewed as an interphase which extends some distance into both phases and is limited to where the material properties are identical to the corresponding bulk phase.

The stress birefringence patterns observed in the single fiber experiment indicate that the strain in the resin—both elastic and plastic—is limited to a narrow region 1–2 fiber diameters around the fiber. On this basis it is reasonable to view the single fiber test as a test of the interphase which clearly extends into the resin and very likely some unknown distance into the fiber subsurface.

The locus of failure within the interphase region determines the level of stress transfer between resin and fiber. It is important to know where this failure occurs. If it is at the fiber resin interface or within the fiber subsurface than it may be possible to improve stress transfer by some physical or chemical modification of the fiber surface. On the other hand, if stress transfer is limited by the shear yield strength of the resin then efforts to modify the fiber surface (or subsurface) properties are likely to be ineffective.

The results reported here for SiC fiber and by Drzal for AU-1

suggest the locus of failure is at or near the fiber surface. In both cases the failure is probably dictated by weak boundary layers on the fiber; a cohesively weak organic finish on the SiC and a weak carbonaceous layer on the AU-1 which can be removed by surface treatment. In the case of AU-4, a slip-stick behavior was observed here (Figure 8) and by Drzal⁵ which suggests a heterogeneous surface where the locus of failure is at the fiber surface or in the subsurface in some regions and a shear yielding of the resin in other regions. Evidence for shear yielding of the resin is based on the residual birefringence after releasing tension on the specimen. This conclusion is subject to some qualification as discussed below.

The locus of failure for the surface treated fibers, AS-1, AS-4, AS-6G and IM-6G is problematical. In the work reported here the birefringence patterns indicate shear yielding of the matrix adjacent to fiber breaks as the specimen is stressed. This would seem to imply that stress transfer is limited by shear yielding of the matrix and not by the fiber-resin interfacial shear strength. However, as pointed out by Drzal¹² because of the difference in Poisson's ratio between fiber and resin a radial compressive stress develops between the fiber and resin which adds a fractional adhesion component to the inherent adhesion between fiber and resin.

Drzal contends that the interfacial shear strength limits stress transfer between fiber and resin for AS-1 and AS-4 in m-PDA/828 resin. This conclusion is based on microtome sectioning of specimens of AS-4 and m-PDA/828. Electron microscopy of sections through a region adjacent to fiber breaks indicated a clean separation between fiber and resin. However, in sectioning through a region in which the resin has been plastically deformed, it is at least possible that in the microtoming operation interfacial separation occurred due to relaxation of the highly stressed resin.

There have been numerous attempts to improve the "adhesion" between carbon fiber and matrix resin. Unfortunately, these studies involved laminate testing which, because of the many variables involved, make interpretation of the results difficult and ambiguous. Drzal⁴ measured τ_c for AS-1 fiber in m-PDA/828 after treatments to reduce the oxygen level (from ESCA) on the fiber surface. A reduction in oxygen of 15–20% had only a marginal effect (~5%) on the interphase shear strength.

CONCLUSIONS

The single fiber-resin tensile test provides a unique means of studying the mechanisms of stress transfer between fiber and resin. Experimental interpretation is aided considerably if the resin is transparent and stress birefringent. For carbon fiber—epoxy systems studied here and by others, fiber breaks can be observed, the critical aspect ratio determined, and the stress condition at and around the fiber breaks revealed by birefringent patterns.

For the fiber-resin pairs studied here, stress transfer was limited either by frictional slip at the interface or a slip-stick adhesion involving intermittent matrix yielding and interfacial failure (the latter could have been cohesive failure within the outer layers of the fiber). There was some indication that stress transfer may also be limited by the shear yield strength of the matrix but the evidence is not unambiguous. Whether the matrix or the interface determine stress transfer is more than an academic question. If stress transfer is limited by the matrix then it is highly unlikely that costly modifications of the fiber surface properties will improve stress transfer or laminate properties where stress transfer is a determining factor, e.g. 0° laminate strength.

A direct correlation was found between laminate 0° tensile strength and the mean critical aspect ratio for production lots of AS-4, AS-6G and IM-6G. This correlation is consistent with the elementary theory of stress transfer that predicts that, *if the fiber-resin shear strength is constant*, then the critical aspect ratio is directly related to fiber tensile strength. Moreover, there is a broad distribution in the measured critical length which is most likely due to the distribution in the flaws that determine fiber strength.

Acknowledgments

The authors wish to thank Mr. Niel Hansen (Hercules Aerospace, Graphite Fiber Development) and Professor L. T. Drzal (Michigan State University) for very helpful discussions during the course of this work.

References

1. A. Kelley and W. R. V. Tyson, *Mech. Phys. Solids* **13**, 329 (1965).
2. W. A. Fraser, F. H. Ancker and A. T. DiBenedetto, *Proc. Conf. on Reinforced Plastics*, SPI Section 22A, p. 1, 1975.

3. W. A. Fraser, F. H. Ancker, A. T. DiBenedetto and B. Elbirli, *Polym. Comp.* **4**, 238 (1983).
4. L. T. Drzal, M. J. Rich and P. F. Lloyd, *J. Adhesion* **16**, 1 (1982).
5. L. T. Drzal, M. J. Rich, M. F. Koenig and P. F. Lloyd, *J. Adhesion* **16**, 133 (1983).
6. L. T. Drzal, *Carbon* **15**, 129 (1983).
7. G. E. Hammer and L. T. Drzal, *Applications of Surface Science* **4**, 340 (1980).
8. ASTM D790-71 (Am. Socy. for Testing & Materials, Philadelphia, PA).
9. S-H. Own, *A Statistical Theory of Interfacial Shear Strength and its Application to Carbon-Fiber Reinforced Polymer Composites*, Ph.D. Dissertation, Washington State University, Pullman, Wash. (1981).
10. Fiber Line Acceptance data base, Hercules, Inc.
11. L. H. Sharpe, *J. Adhesion* **4**, 51 (1972).
12. L. T. Drzal, personal communication.